AD-A180 250 AN EXPERIMENTAL INVESTIGATION OF THE KINEMATICS OF BREAKING WAVES(U) FLOW RESEARCH CO KENT WA J H DUNCAN ET AL. APR 87 FLOW-RR-400 N00014-84-C-0698 1/1

UNCLASSIFIED F/G 20/4 NL

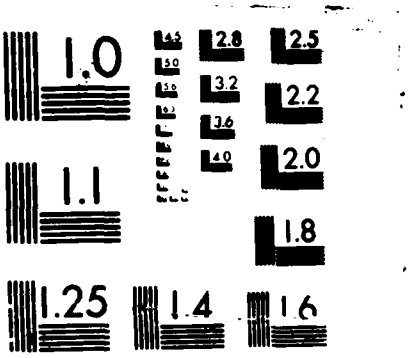

Flow Research Report No. 408

(2)

AN EXPERIMENTAL INVESTIGATION OF THE KINEMATICS OF BREAKING WAVES

J. H. Duncan
Flow Research Company
1320 Fenwick Lane, Suite 401
Silver Spring, Maryland 20910

L. A. Wallendorf and B. Johnson
Hydromechanics Laboratory
The United States Naval Academy
Annapolis, Maryland 21402

April 1987

Prepared for
The United States Coast Guard
and
The Office of Naval Research
Under Contract N00014-84-C-0698

FLOW RESEARCH COMPANY
Applied Mechanics Division
21414-68th Avenue South
Kent, Washington 98032
(206)872-8500

AN EXPERIMENTAL INVESTIGATION OF THE KINEMATICS OF BREAKING WAVES

J. H. Duncan
Flow Research Company
1320 Fenwick Lane, Suite 401
Silver Spring, Maryland 20910

L. A. Wallendorf and B. Johnson
Hydromechanics Laboratory
The United States Naval Academy
Annapolis, Maryland 21402

Summary: An experimental investigation of the evolution of the profiles of a set of spilling and a set of plunging breaking waves is presented. Each set of waves consists of similar waves scaled to three characteristic wave periods. Measurements of various wave heights, periods, and phase speeds are presented.

1. Introduction

Breaking waves are important in many oceanographic phenomena and in the design of marine structures and vehicles. In oceanography, wave breaking provides a mechanism in which wind generated waves transfer their energy to turbulence. This turbulence enhances the transfer of heat and gases across the air-sea interface. The forces produced by breaking waves on ships and marine structures can also be of great importance. At the instant that the wave breaks, the fluid velocities near the crest are about equal to the wave phase velocity. The momentum of this mass of water can produce impact pressures that are capable of capsizing boats and damaging marine structures.

In order to study any of the above phenomena in the laboratory, one must first produce a set of waves that cover an appropriate range of sizes and types to drive the phenomena under study. This is not a simple task because breaking waves are not well understood. Fundamental to this problem is the identification of a simple set of independent variables that quantitatively describe a breaking wave. In the case of steady, periodic, nonbreaking waves, the independent variables have been known since the original work of Stokes (1847). Here the wave is completely described by two independent variables, either its period and amplitude, or its wavelength and amplitude. In the breaking-wave case, the wave profile evolves as it propagates changing in period and amplitude until the crest either spills or plunges forward. This evolution can be driven by varying water depth, interaction with a mean current, or, as in the present experiments, interaction with other components in a wave packet. The variables that completely describe these waves are not known. It seems reasonable that one of these would be the apparent period of the wave at the time it begins to break. As in the steady wave case, the period should be related to the wavelength (but probably in some complex way), thus determining the general length scale of the wave. For a wave with a given period at the point of incipient breaking, it is thought that one or more variables will determine the breaker type which can range from a gentle spiller to a plunging breaker. These variables might include wave slope and asymmetry parameters at the time of breaking, as well as parameters that depend on the time history of the wave profile (for

example, the rate of increase of wave height or steepness).

There are two goals in the present experimental research program. First, we wish to develop a technique for generating a given breaker type at various wave periods with a single wavemaker. These waves could then be used in subsequent studies to test, for instance, the capsize resistance of boat models in the presence of several plunging and spilling breakers as a function of wave period. Our second goal is to search for a set of independent variables that describe these waves and, in particular, to find quantitative measures that indicate the occurrence of breaking and the breaker type. Several papers in which the profiles of breaking waves have been studied quantitatively have appeared in the recent literature (Bonmarin and Ramamonjiarisoa , 1984, Kjeldsen and Myrhaug, 1979, and Melville and Rapp, 1985). In the present study we expand upon this previous work by examining one spilling and one plunging breaking wave, each of which is scaled to three absolute wave periods.

2. Experimental Details.

2a. Facilities.

The experimental research program was conducted in a wave tank at the United States Naval Academy. The tank is 36.6 m in length, 2.44 m wide and 1.5 m deep. It is equipped with an MTS dual flap wavemaker which is 2.44 m wide and 1.83 m high, extending the full tank depth. A hydraulic actuator is used to drive the lower wave board with respect to the tank foundation; a second actuator is used to drive the upper wave board with respect to the lower wave board.

2b. Wave Height Measurments.

Wave profile measurements were obtained with four linear resistance wave height gauges. The gauges were mounted 20 to 30 cm apart along the tank centerline on a movable platform. For each wave, measurements were taken with the platform at 5 separate positions, resulting in wave records at 14 locations. Positions were chosen ranging from a small distance past the break point to about one wavelength toward the wavemaker from the break point. The heights of the wave crest and troughs, and the various wave periods were measured from each single wave record. Using the probe pairs, the speeds of the crest, troughs, and zero crossings were computed. Measurements were repeated three times; reported values are the average of these results.

3. Wavemaker Driving Signal

The computer program that generated the driving signal for the wavemaker was a modification of the program used by Salsich et al (1983). The purpose of the modifications was to facilitate the scaling of a given driving signal to various frequencies. In its modified form, the program generates a signal that can be divided into two basic segments. In the first segment, both the frequency and amplitude of the signal were held constant. During this period, the wavemaker hydraulic system was brought up to full stroke while producing a few very small amplitude waves. In the second segment, the frequency was decreased linearly with time. The sweep in the frequency during this segment causes the wave pattern to converge since the lower frequency waves overtake the slower waves generated ahead of them. By linear theory (Longuet-Higgins 1974) the

distance from the wavemaker to the point where the waves converge is given by

$$X_b = -\frac{g}{4\pi\, df/dt} \tag{1}$$

where f is the frequency in hertz, t is time and g is the acceleration of gravity. Wave breaking occurs at some distance from the wavemaker which is less than X_b. The amplitude of the signal is also varied as the frequency is varied. As the frequency decreases from f_1, its initial value, to an intermediate frequency, f_p, the amplitude is increased. Then, as the frequency continues to decrease to f_2, the amplitude decreases to its original value. In order to describe this amplitude envelope, we first define a frequency, f_i, during the time when the frequency is between f_1 and f_p:

$$f_i = f_1 + \frac{(f_1 - f_{av})}{(f_1 - f_p)}(f - f_1) \tag{2}$$

Note that

$f_i = f_1$ at $f = f_1$

and

$f_i = f_{av}$ at $f = f_p$.

where $f_{av} = 0.5(f_1 + f_2)$.

The amplitude of the wave envelope during this phase of the signal is then given by

$$A_i = \exp\left\{ E\,\frac{(f_{av} - f_i)}{f_{av}} \right\}\left(\frac{f_{av}}{f_i}\right)^P \tag{3}$$

where E and P are positive constants. Between frequencies f_p and f_2 another frequency, f_d, is defined:

$$f_d = f_2 + \frac{(f_2 - f_{av})}{(f_2 - f_p)}(f - f_2) \tag{4}$$

Note that

$f_d = f_{av}$ at $f = f_p$

and

$f_d = f_2$ at $f = f_2$.

The amplitude of the wave envelope in this region is given by

$$A_d = \exp\left\{ E\,\frac{(f_d - f_{av})}{f_{av}} \right\}\left(\frac{f_{av}}{2f_{av} - f_d}\right)^P \tag{5}$$

The amplitude functions have the properties: $A_i(f_1) = A_d(f_2)$, and $A_i(f_p) = A_d(f_p) = 1.0$.

In the study described below, we have chosen a set of values for E, P, f_p/f_1, and f_2/f_1 and scaled the wave generation signal to several values

of absolute frequency, say f_p. Given the above parameters, we then adjust the theoretical break point, X_b, in each case to create the same number of waves in the generation signal. Let the variables describing two scaled wave signals be distinguished by ′ and ″. The first step in making the signals similar is to scale the three frequencies (f_1, f_p, and f_2) by the same ratio:

$$f_1''/f_1' = f_p''/f_p' = f_2''/f_2' = \alpha. \tag{6}$$

Since the frequency is the number of waves passing a given point per unit time, the number of waves generated, n, is given by the integral of the frequency over time. Thus,

$$n = \int_0^{t_2} f \, dt = \int_0^{t_2} f_1 + \frac{df}{dt} t \, dt \tag{7}$$

where df/dt is given by Equation (1) and t_2 is obtained from

$$\frac{f_2 - f_1}{t_2 - 0} = \frac{df}{dt} \tag{8}$$

After performing the integration and some algebraic manipulation, Equation (7) becomes

$$n = \frac{2\pi X_b}{g} (f_1^2 - f_2^2) \tag{9}$$

Since the number of waves in the two wave trains is to be the same we have

$$1 = \frac{X_b'}{X_b''} \frac{(f_2'^2 - f_1'^2)}{(f_2''^2 - f_1''^2)} \tag{10}$$

Or using Equation (6)

$$\frac{X_b'}{X_b''} = \alpha^2. \tag{11}$$

Because the transfer function between the wavemaker and the waves generated is a nonlinear function of frequency, one would not expect the wavetrains generated by these scaled driving signals to have exactly the same scaled profiles. However, due to the preliminary nature of this study, no attempt to account for these nonlinearities was made. The results presented below indicate that within the range of frequencies used, the scaling procedure was adequate.

4.Results and Discussion

The waves used in this study were produced with one type of wavemaker driving signal. The parameters for this signal were f_p/f_1=0.70, f_2/f_1=0.60, E = 5.0, and P = 4.0. A plot of the signal appears in Figure 1. This signal was scaled to three different frequencies (f_p =0.70, 0.85, and 1.0). For each frequency, two amplitudes of the signal were chosen so that the wave broke at x/X_b= 0.67 and 0.80, where x is the distance from the wavemaker; the breaking events at x/X_b= 0.80 were spilling breakers, while the breaking events at x/X_b= 0.67 were plunging breakers. These

results are consistent with Salsich et al (1983). When the signals were first input to the wavemaker, two breaking events sometimes occurred near the desired point of incipient breaking (break point). This problem was remedied by varying the phase of the drive signal within the envelope described by equations (3), and (5) until a single breaking event occurred.

A set of wave profiles taken at four positions near the break point for one of the waves appears in Figure 2. Wave profiles such as these, measured within one wavelength of the break point, were used to study the behavior of the wave as it approached breaking.

The most fundamental parameter of interest is the wave period measured by a single probe. A sketch showing the definitions of the various features of the breaking wave profile is given in Figure 3. The wave period, T_d, is defined as the time between the passage of the downward zero-crossing of the trough ahead of the breaker and the downward zero-crossing of the breaking crest ($T_d = T_5 - T_1$). A second wave period, called the crest period, T_c, is defined as the time between the passage of the upward zero-crossing ahead of the breaking crest and the downward zero-crossing after the crest ($T_c = T_5 - T_3$). Figure 4a contains a plot of these wave periods versus distance, x, from the nominal break point for the three spilling breakers, and Figure 4b contains the data for the three plunging breakers. The horizontal distance, x, is scaled by the wavelength, L_o, of a linear wave whose period, T_o, equals the value of T_d at the break point in each case. The break point, which is near $x = 0$, was chosen based on the plots of crest height versus distance from the break point (see below). The periods are nondimensionalized by the appropriate T_o. Notice that in all six cases both periods decrease slowly as the break point is approached. In the vicinity of the break point, T_d reaches a minimum and then increases, while T_c becomes nearly constant. The significance of this minimum is not known. The collapse of the data with the above scaling is excellent for the spilling breakers and good for the plunging breakers.

The height of the crests of the breakers, η_c, and the depths of the preceding and the following troughs, η_{tp} and η_{tf}, are plotted versus horizontal distance from the break point in Figure 5a for the spilling breakers and in Figure 5b for the plunging breakers. All variables are nondimensionalized by the appropriate value of L_o for each wave. The height of the crest increases as the break point is approached. In all but one case, the plunging breaker with $f_p = 1.0$, the crest height reaches a maximum at the point where the wave visually appears to break. This is in agreement with the experimental results of Bonmarin and Ramamonjiarisoa (1984) and the numerical results of Longuet-Higgins and Cokelet (1976). The point where the height of the crest reached a maximum was chosen as the point of incipient breaking (break point) in those five cases. In the sixth case, the plunging breaker with $f_p = 1.0$, the data point with the smallest x was taken as the break point. Thus, the break point was between 0 and 0.1 x/L_o in all cases. With the exception of the plunging breaker with $f_p = 1.0$, the data collapses quite well. The dimensionless wave height, η_c/L_o, at the break point for the spilling breakers was about 0.08, while for the two scaled plunging breakers it was 0.09. In much of the data, the results for the plunging breaker with $f_p = 1.0$ differ from the other two plungers. The reason for this discrepancy is assumed to be experimental error, however, there was insufficient time prior to the present publication date to explore this problem further.

As the break point is approached, the depth of the trough preceding the breaking crest decreases, while the opposite occurs for the following trough. Bonmarin and Ramamonjiarisoa (1984) report a qualitatively similar behavior for the preceding trough in their experiments. The curves for the preceding and following troughs cross at $x/L_o = 0.1$ for the spilling breakers and $x/L_o = 0.35$ for the plunging breakers. The total wave height based on the preceding trough increases slightly as the break point is approached, reaching $0.11\ L_o$ and $0.12\ L_o$ for the spilling and plunging breakers, respectively.

Three dimensionless parameters that quantify the asymmetry of the wave form ($s_{c'}$, μ_H, and μ_v, see IAHR 1986) are plotted versus x/L_o in Figure 6a for the spilling breakers and in Figure 6b for the plunging breakers (see Figure 3 for definitions). These parameters were first used by Kjeldsen and Myrhaug (1979) who called them ε, μ, and λ, respectively. The crest front steepness, $s_{c'}$, can be considered as the ratio of the average rise velocity of the water surface (from the time of passage of the upward zero-crossing ahead of the crest to the time of passage of the crest), divided by the celerity of a linear wave based on the period, T_d. The parameter $s_{c'}$ increases slowly up to the break point and then decrease for all but the plunger with $f_p = 1.0$. The average value at the break point is about 0.50 for the spilling breakers and 0.70 for the plunging breakers. Kjeldsen and Myrhaug (1979) found $s_{c'}$ in the range 0.32 to 0.78 in their laboratory data, while Bonmarin and Ramamonjiarsoa (1984) found a maximum $s_{c'}$ of 0.55 in their investigation of a single wave.

The asymmetry parameter μ_H is the ratio of the crest height, η_c, to the vertical distance between the preceding trough and the crest, $\eta_c - \eta_{pt}$. It is a measure of the asymmetry of the profile about the horizontal axis. This parameter continually increases for all waves and has an average value of about of 0.75 for both the spillers and the plungers at the break point. Thus, for the waves studied, it seems that a value of μ_H near 0.75 may indicate the occurence of a breaking event, while the value of $s_{c'}$ at that instant may indicate the breaker type.

The last asymmetry parameter, μ_v, is a measure of the asymmetry of the profile of the wave crest about a vertical axis. It is defined as the ratio of the time delay between the passage of the crest and the following downward zero-crossing to the time delay between the preceding upward zero-crossing and the crest. This parameter increases at first and reaches a maximum a little ahead of the break point in all cases except the plunging breaker with $f_p = 1.0$. The average peak value is about 1.9 for the plunging breakers and 1.8 for the spilling breakers. At the break point, μ_v has decreased to 1.7 and 1.3 for the plunging and spilling breakers, respectively.

Plots of the horizontal speed of the crest, c_c, divided by the speed of the upward zero-crossing preceding the crest, c_3, and c_c divided by the speed of the downward zero-crossing following the crest, c_5, versus horizontal position are given in Figures 7a and 7b for the spilling and plunging breakers, respectively. The speeds were obtained by measuring the time delay in the passage of the feature in question at two wave height probes with a known distance between them. These phase speed ratios indicate the average rate of steepening of the forward and rear face of the wave crest. When $c_c/c_3 > 1$, the forward face of the wave is steepening, while the rear face of the wave steepens when $c_c/c_5 < 1$. Note from Figure 2 that the average steepness or slope is considerably less

than the instantaneous slope near the crest just prior to breaking. The curves in Figure 7 are jagged due to the magnification of small errors when subtracting the time of passage of a given feature at neighboring probes; however, some general trends can be seen in the data. For both the spilling and plunging breakers, the forward and rear faces of the wave are steepening slowly for large x ($c_c/c_3 \gtrsim 1.0$, $c_c/c_5 \gtrsim 1.0$). As x decreases, c_c/c_5 decreases steadily; concurrently, c_c/c_3 at first increases and then decreases. At the break point, c_c/c_5 and c_c/c_3 are nearly equal with a value of 0.8 and 0.9 for the spilling and plunging breakers, respectively.

5. Conclusion

The collapse of the data for the three spilling and the three plunging breakers indicates that the proposed method is capable of generating a given breaker type at a range of wave periods. In future work, attempts will be made to improve the accuracy of the method by accounting for the nonlinearity of the transfer function of the wavemaker. The analysis of various wave profile parameters measured with single wave height probes indicates that the horizontal asymmetry factor, μ_H, may be the best indicator of the occurrence of a breaking wave. It increased steadily to about 0.75 at the point of incipient breaking for the six waves investigated herein. During the beginning of the breaking process it continued to increase. The crest front steepness, $s_{C'}$, also increased as the wave approached the point of incipient breaking. It then decreased during the beginning of the breaking process. Its value at the break point was 0.50 for the spilling breakers and 0.70 for the plunging breakers. Thus, the value of $s_{C'}$, at the instant when $\mu_H = 0.75$ may be a good indicator of breaker type. The use of two-probe arrays for detecting breaking events from wave phase speeds will require improvements in the accuracy of the measurements.

Acknowledgements:

This work was supported by the United States Coast Guard, Naval Engineering Division, under the direction of Steven H. Cohen, and the David Taylor Naval Ship Research and Development Center, Code 1561, under the direction of Susan Bales. We also acknowledge the work of Alan Engle of NAVSEA who began a similar investigation of a single breaking wave while working as an Engineer in Training at the USNA Hydromechanics Laboratory.

References:

Bonmarin, P. and Ramamonjiarisoa, A. 1984, "Deformation to Breaking of Deep Water Gravity Waves", Experiments in Fluids, 2, pp. 1-6.

International Association for Hydraulic Research, 1986 "List of Sea State Parameters," Supplement to Bulletin No. 52(1986), Brussels, Belgium.

Longuet-Higgins, M. S. 1974 "Breaking Waves in Deep and Shallow Water", Proc. 10th Symp. Naval Hydrodynamics, Boston, Mass.

Longuet-Higgins, M. S. and Cokelet 1976 "The Deformation of Steep Waves on Water. I. A Numerical Method of Computation", Proc. Roy. Soc. Lond. A 350, pp. 1-26.

Mellville, M. K. and Rapp, R. J. 1985 "Momentum Flux in Breaking Waves" Nature, 317, No. 10, pp. 514-516.

Myrhaug, D. and Kjeldsen, P. 1983 "Parametric Modelling of Joint Probability Density Distributions for Steepness and Asymmetry in Deep Water Waves," J. Coastal Eng., Amsterdam.

Salsich, J.O., Johnson, B. and Holton, C. 1983 "A Transient Wave Generation Technique," Proc. 20th ATTC, Hoboken, N.J.

Stokes, G.G. 1847 "On the Theory of Oscillatory Waves," Trans. Camb. Phil. Soc. 8, 441-55; reprinted in Math. Phys. Pap I, 314,26.

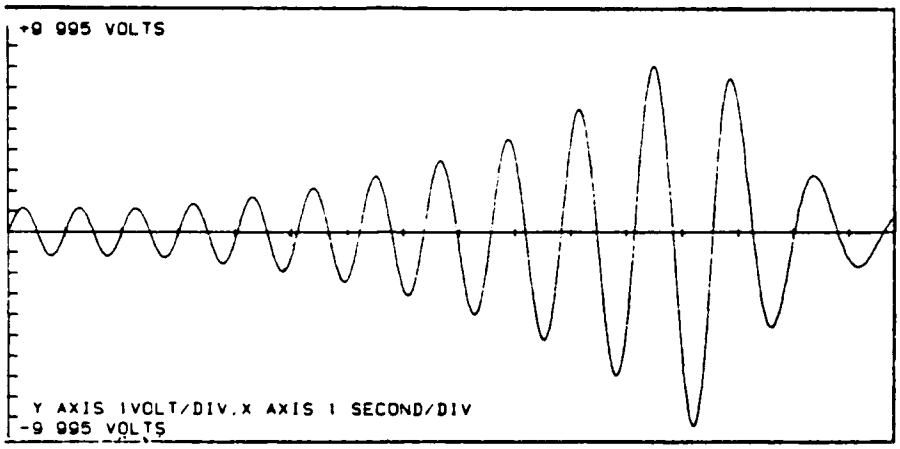

FIGURE 1 Example Wave Maker Drive Signal

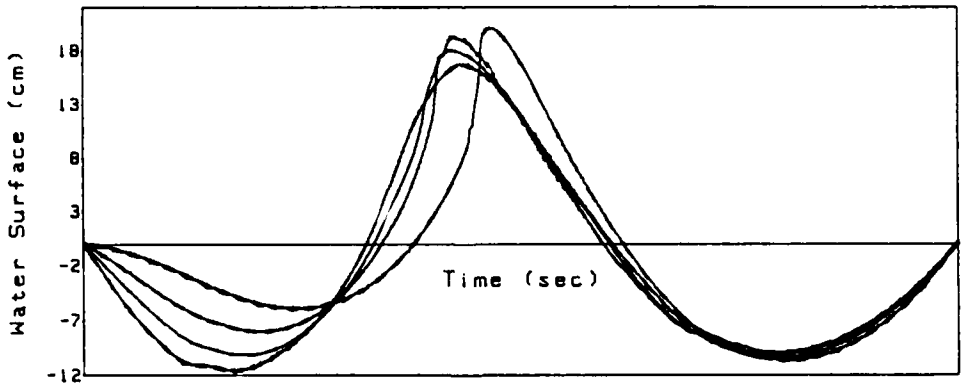

FIGURE 2 Wave Profiles Near the Breakpoint (f_p =0.70 hz.)

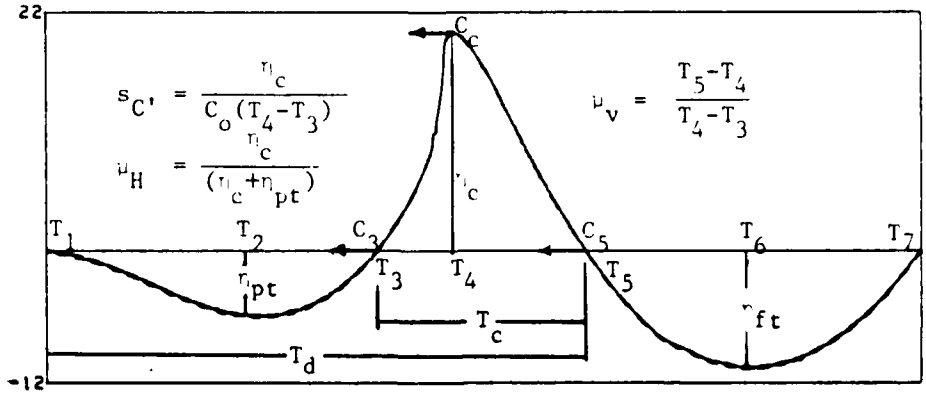

FIGURE 3 Definition of Breaking Wave Profile

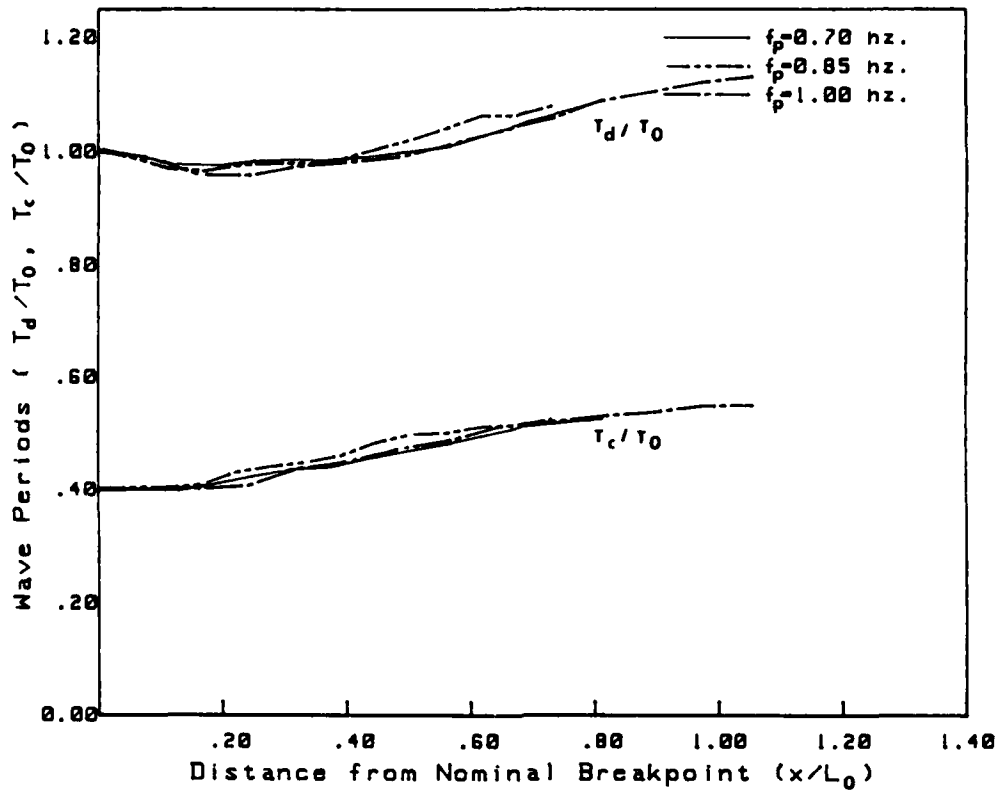

FIGURE 4a Wave Periods - Spilling Breakers

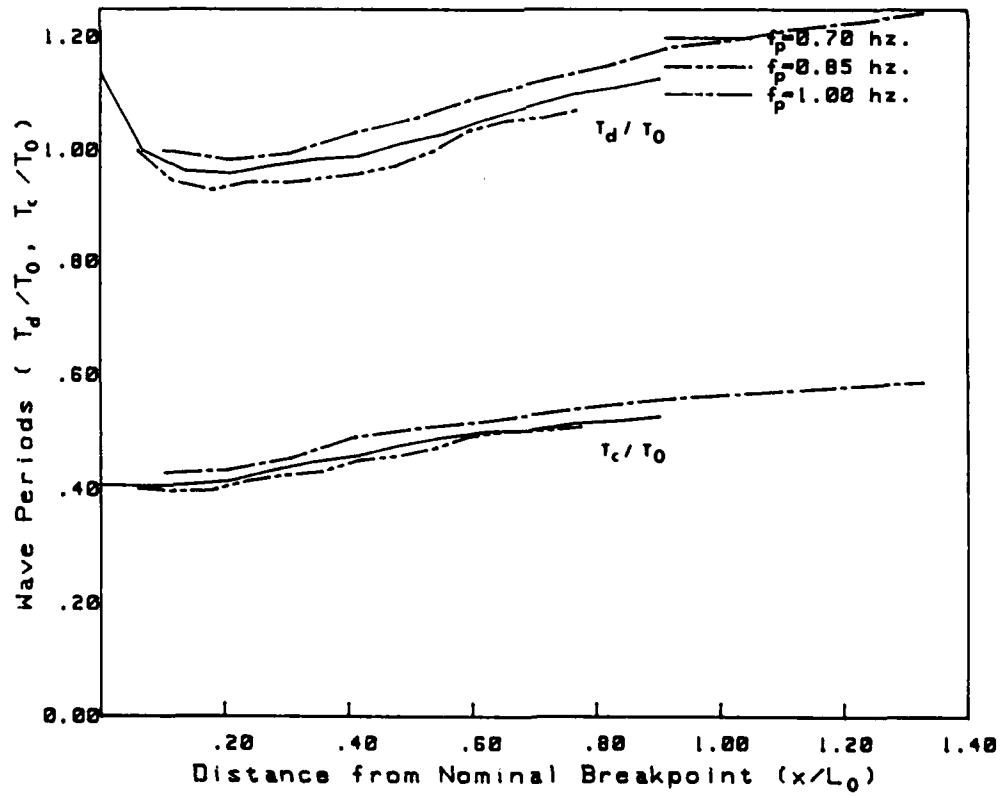

FIGURE 4b Wave Periods - Plunging Breakers

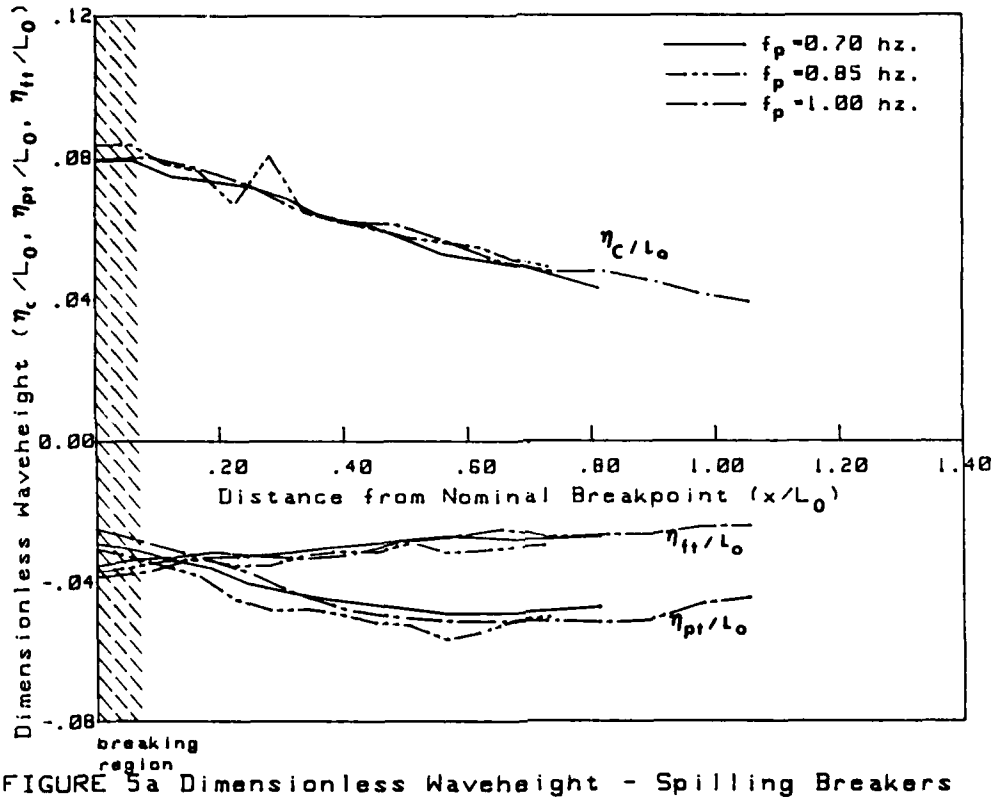

FIGURE 5a Dimensionless Waveheight - Spilling Breakers

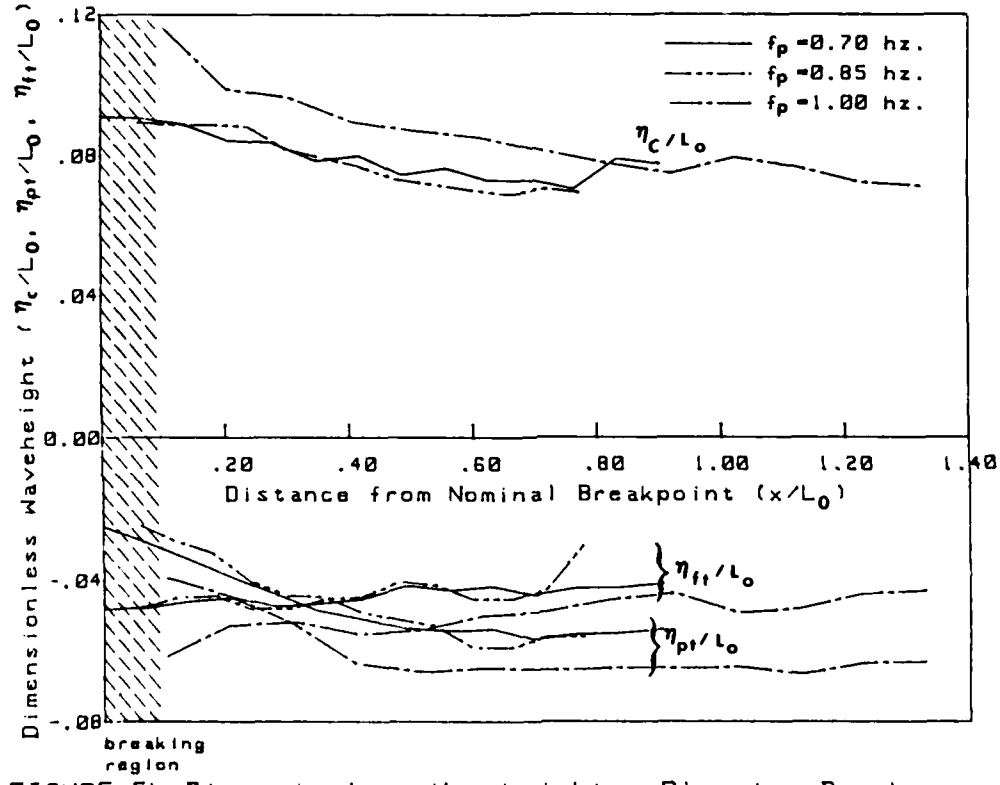

FIGURE 5b Dimensionless Waveheight - Plunging Breakers

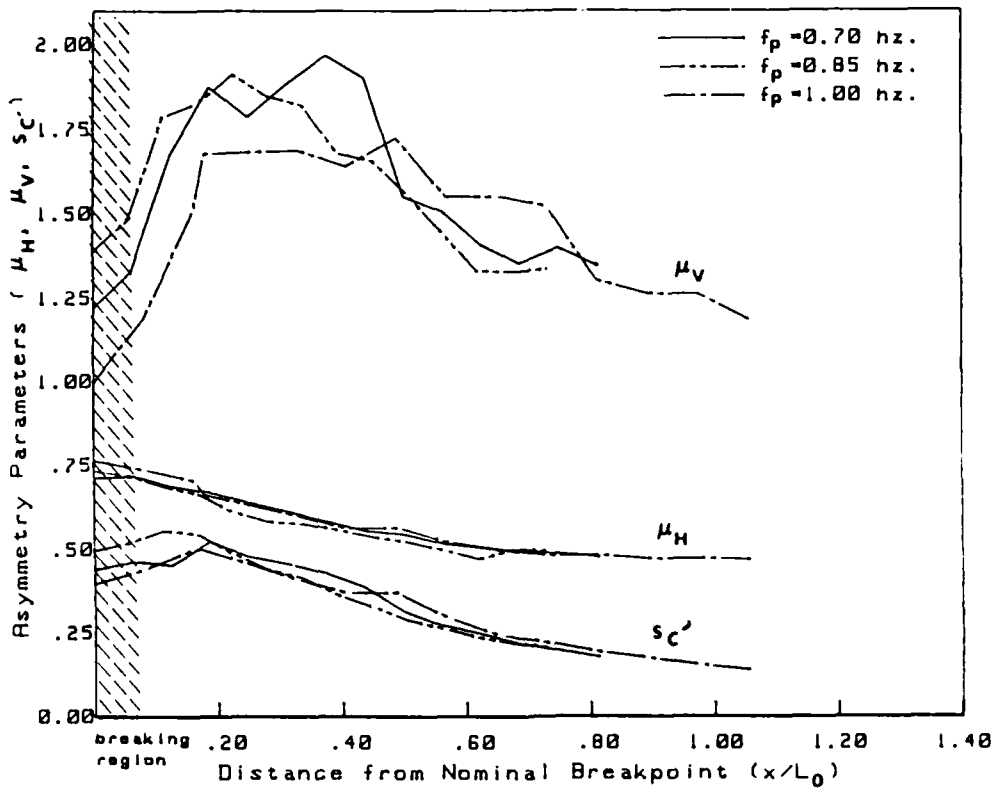

FIGURE 6a Asymmetry Parameters (Kjeldsen & Myrhaug, 1979)- Spilling Breakers

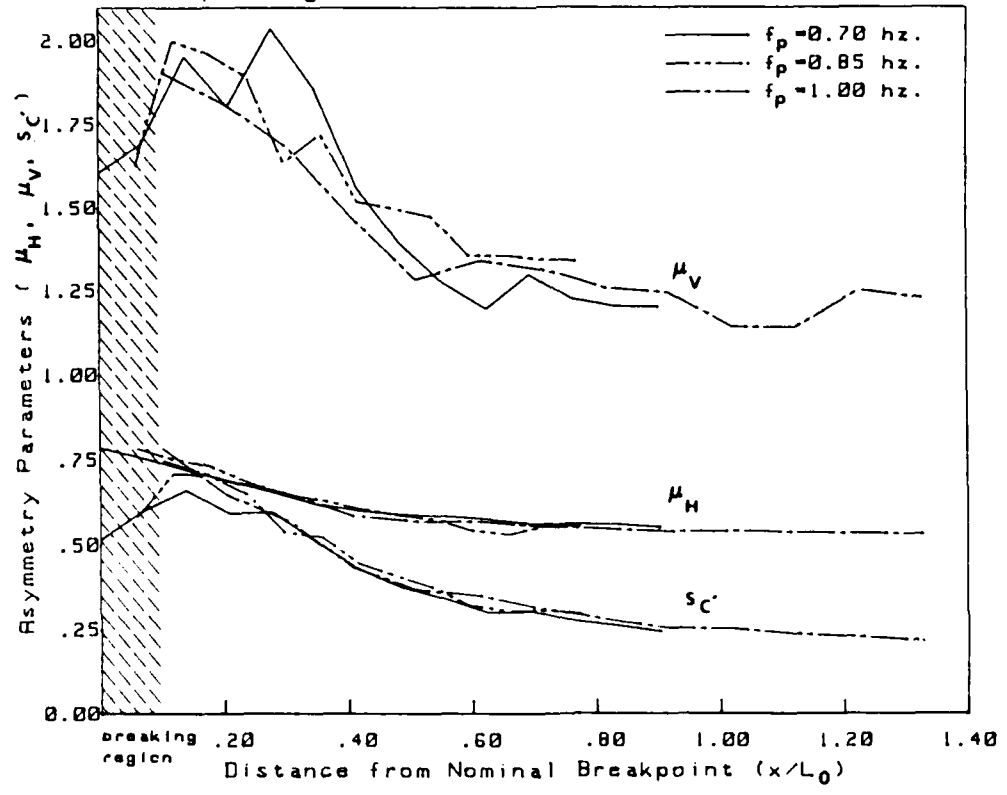

FIGURE 6b Asymmetry Parameters (Kjeldsen & Myrhaug, 1979)- Plunging Breakers

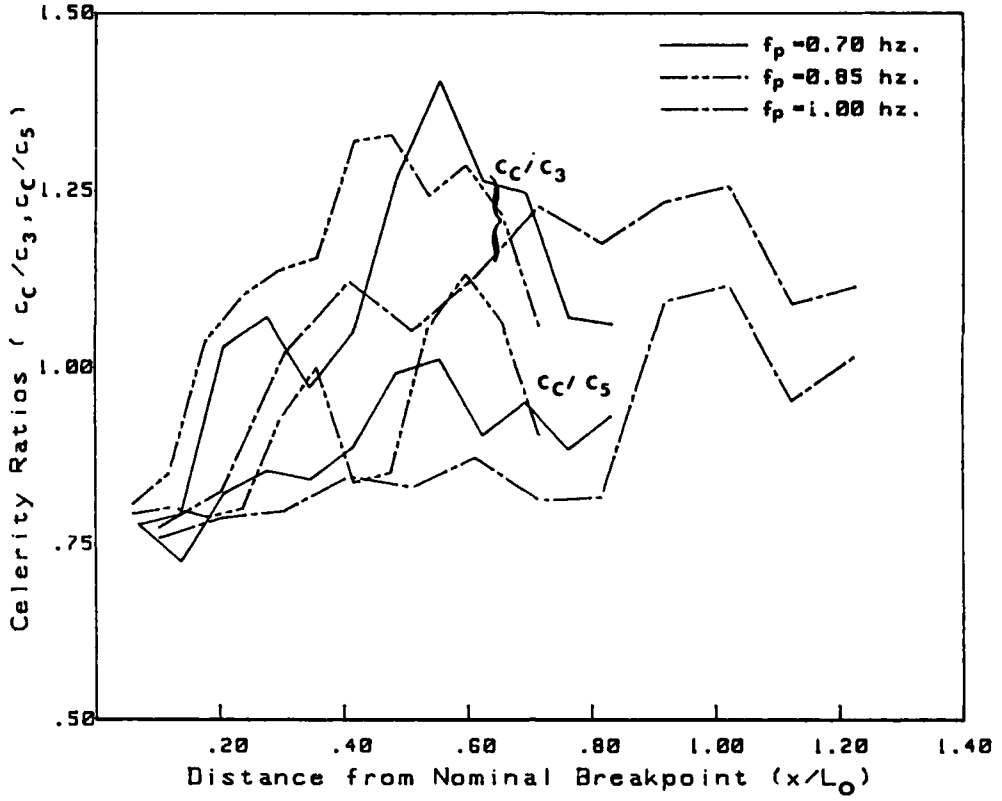

FIGURE 7a Wave Celerity Ratios - Spilling Breakers

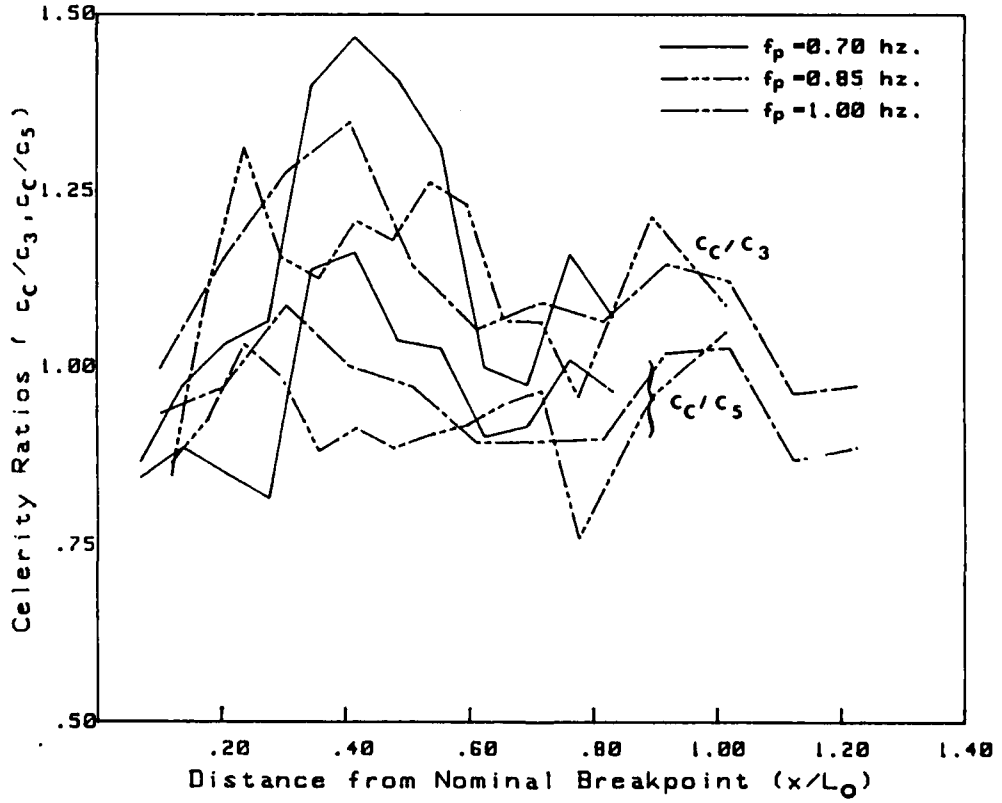

FIGURE 7b Wave Celerity Ratios - Plunging Breakers

END

6-87

DTIC